NASA Technical Memorandum 101474
AIAA-89-0004

Three Dimensional Viscous Analysis of a Hypersonic Inlet

D.R. Reddy, G.E. Smith,
and M.-F. Liou
Sverdrup Technology, Inc.
NASA Lewis Research Center Group
Cleveland, Ohio

and

T.J. Benson
National Aeronautics and Space Administration
Lewis Research Center
Cleveland, Ohio

Prepared for the
27th Aerospace Sciences Meeting
sponsored by the American Institute of Aeronautics and Astronautics
Reno, Nevada, January 9-12, 1989

NASA

THREE DIMENSIONAL VISCOUS ANALYSIS OF A HYPERSONIC INLET

D.R. Reddy,* G.E. Smith,** and M.-F. Liou**
Sverdrup Technology, Inc.
NASA Lewis Research Center Group
Cleveland, Ohio 44135

and

T.J. Benson***
National Aeronautics and Space Administration
Lewis Research Center
Cleveland, Ohio 44135

ABSTRACT

The flow fields in supersonic/hypersonic inlets are currently being studied at NASA Lewis using two- and three- dimensional full Navier-Stokes and Parabolized Navier-Stokes solvers. These tools have been used to analyze the flow through the McDonnell Douglas Generic Option 2 inlet which has been tested at Calspan in support of the National Aerospace Plane Program. Comparisons between the computational and experimental results are presented. These comparisons lead to better overall understanding of the complex flows present in this class of inlets. The aspects of the flow field emphasized in this work are the three-dimensional effects, the transition from laminar to turbulent flow, and the strong nonuniformities generated within the inlet.

INTRODUCTION

Accurate prediction of hypersonic inlet flow fields is essential for the overall performance evaluation of high speed propulsion systems. Since the inlet is the first component in the propulsion system, its performance influences the performance of the downstream components and consequently, the performance of the entire system. Various types of problems can be encountered in inlet flow fields. The flow can separate, strong secondary flows can develop as a result of shock/boundary layer interactions, and the inlet can go into a shock wave oscillation cycle known as buzz.

In order to simulate the inlet flow field, two numerical codes, each belonging to a different class of algorithms, have been selected. The two codes , a time-marching full Navier-Stoke (NS) code, PARC[1], and a space marching Parabolized Navier-Stokes (PNS) code, PEPSIS[2], have been extensively verified in the supersonic and hypersonic regimes. Two dimensional[3,4,5], axisymmetric[3,6], and 3-D[7,8,9] calculations and comparisons with experiment have been performed using the PARC code. Similar comparisons using PEPSIS, for 2-D[10] flows and 3-D corner[10] and inlet[11,12] flows have also been performed.

The PARC code solves the Reynolds-averaged Navier-Stokes equations in strong conservation form with the Beam and Warming approximate factorization algorithm[13]. It uses central differencing and Jameson type explicit and implicit artificial dissipation[14]. To simplify the solution of the resulting block pentadiagonal system, the block implicit operators are diagonalized thereby reducing the equations to a scalar diagonal system[15]. The loss of time accuracy due to the diagonalization does not affect the spatial accuracy of the solution[15]. This code was originally developed as AIR by Pulliam and Steger[16]. Pulliam[15] later added the Jameson[15] artificial dissipation and called the code ARC. Cooper[1] adapted the ARC code for internal flow problems in propulsion applications and named the code PARC.

In regions of the flow not dominated by elliptic effects, single sweep PNS flow solvers can be employed with minimal loss of accuracy. In fact greater flow field resolution can be obtained since finer grids are possible as a result of reduced computational effort compared to NS solvers. The class of internal flows found in hypersonic inlets performing at or near design conditions is generally free of elliptic effects except for small areas of subsonic flow near the walls of the inlet. The PEPSIS code solves the steady parabolized Navier-Stokes (PNS) system of equation for hypersonic or supersonic flow using a linearized block implicit scheme. Special treatment of the equations prevents branching in the subsonic portion of the flow field. The solution is obtained by spatially marching in the dominant flow direction.

The Generic Option 2 inlet tests were conducted to support the National Aerospace Plane program. The original test matrix included flow conditions that were fully laminar, transitional and fully turbulent. Prior to inlet testing, PNS calculations were made for the turbulent flow conditions at Mach 11.3. Because of scheduling problems, only the transitional flow condition at Mach 12.25 was tested experimentally. There was not enough time to rerun all the calculations at Mach 12.25. Consequently, results are presented from PARC for laminar flow at Mach 12.25 and from PEPSIS for turbulent flow at Mach 11.3. Transitional flow was not simulated since an appropriate eddy viscosity model does not exist at this time.

---

* Supervisor Turbomachinery Analysis, Member AIAA
** Research Engineer, Member AIAA
***Research Engineer

RESULTS AND DISCUSSION

EXPERIMENTAL CONFIGURATION

The experimental inlet is a scaled down model of the Generic Option 2 hypersonic inlet which has been tested[17] by the McDonnell Douglas Corporation. The total pressure and temperature at the entrance to the model were 3388.9 psi and 3420.7°R respectively. The entrance Mach number was 12.25 and the Reynolds number per foot was 1.05E06. The duration of the test was 30 msec out of which a steady state was observed for the last 15 msec. The geometry of the Generic Option 2 inlet is shown in Figure 1. The inlet is located 30 inches from the leading edge of the flat plate in order to simulate the boundary layer growth on the forebody of a hypersonic aircraft. Top and bottom compression wedges slow the incoming flow through a series of oblique shock waves. The contraction of the inlet can be varied, although the present calculations and experiments have all been run at a contraction ratio of 5.0. Side plates swept at 45° connect the top and bottom wedges and prevent compressed flow from spilling over the sides of the inlet. The three fuselage stations shown in Figure 1 correspond to the locations where the comparisons with experiment will be made. For the comparisons labeled outboard, the static and pitot pressure rakes are located .375 and .625 inches from the sidewall, respectively.

COMPARISON WITH EXPERIMENT

Comparisons between predictions and experimental data were made using results from a two-dimensional analysis (PARC2D) and a three-dimensional analysis (PARC3D). In both cases the flow was assumed to be laminar. This assumption was verified by the experimental investigators[17] for a majority of the flow in the inlet. However, discussions with Cosner[18] of McDonnell Douglas and the heat transfer data in Reference 17 indicated that the flow in the corners of the inlet was transitioning from laminar to turbulent. Since it was not possible to simulate this transition, the fully laminar predictions are presented.

The 3-D computations were done on the CRAY-2 computer at NASA Ames using a grid size of 150 x 81 x 41. The 2-D computations were performed on a 150 by 81 grid on the CRAY-XMP at NASA Lewis. Both results are presented to highlight the difference between 3-D and 2-D flow fields.

Figure 2 shows the static pressure distribution on the ramp surface along the center line of the inlet. The comparison of the PARC3D solution with the experimental data shows good agreement throughout the length of the duct. The solution from PARC2D does not compare well with the data due to three-dimensional effects present in the inlet. The pressure from the 3-D calculation is higher due the coalescence of secondary flow from the sidewalls along the ramp centerline. The pressure distribution on the cowl surface along the centerline is shown in Figure 3. The PARC3D solution once again compares well with the experimental data. However, there are no data points in the middle of the duct where the solution shows a peak in the pressure. The PARC2D solution departs from the experimental values beyond 50 inches due to the three-dimensional nature of the flow.

Figures 4 and 5 show the pressure distribution on the ramp and cowl surfaces on the outboard side of the inlet, thus only the 3-D calculations are shown. The calculated ramp surface pressures in Figure 4 are in good agreement with the experiment. Both the trends and the magnitude are in good agreement. The agreement between PARC3D solution and the cowl surface pressure data shown in Figure 5 is rather poor. The reason for this discrepancy is believed to be the turbulent transition of the flow near the corners of the inlet even though the bulk of the flow though the inlet is laminar.

Figure 6 shows the pitot pressure profile at the entrance of the inlet. The rise in the pitot pressure ratio (>1.0) is due to the shock coming from the flat plate preceding the entrance of the inlet. The numerical smearing of the shock makes the pitot pressure distribution slightly smoother than the sharp change of the profile which resulted experimentally. However, the level of the profile averaged over the height of the duct above the shock agrees well with the data. The effect of slight shock smearing can also be seen in the pitot pressure profile at the fuselage station 40.0 inches from the leading edge of the flat plate (designated F-S 40.0) which is shown in Figure 7. The middle portion of the duct, which would have a free stream value in the presence of sharper shocks from the ramp and the cowl, shows a slightly higher value than the free stream value. However, the solution agrees well with the single data point above the cowl shock towards the cowl surface. The numerical smearing may be a result of the grid resolution and the artificial viscosity model in PARC. Currently there is no mechanism for reducing the artificial viscosity in areas where it is not required such as near walls and in areas of high grid resolution.

Figure 8 shows the pitot pressure profile at F-S 51.7 which is the final constant area portion of the inlet. Comparison of the solution with the data is poor close to the cowl surface; however, away from the wall the agreement is reasonable. The poor comparison close to the wall can be attributed to a lack of grid resolution and to artificial dissipation. Further studies with a different grid distribution and some modifications to the artificial dissipation model, such as reducing the artificial dissipation in the boundary layer, should be performed. Finally, the pitot pressure profile at F-S 51.7 on the outboard side of the inlet is shown in Figure 9. The solution does not agree well with the experimental data, possibly due to the turbulent transition of the flow near the corners.

PREDICTED FLOW FIELD FEATURES

Figure 10 shows Mach number contours from the PARC3D calculations at Mach 12.25 for several planes inside the inlet. The flow enters the inlet at the right and is deflected upward by the ramp shock. Six inches further downstream the flow encounters the cowl lip shock which deflects the flow downward. The boundary layers formed on the swept sidewall interact with the shocks from the ramp and cowl surfaces causing the boundary layer to thin in the corners formed by the compression surfaces and the sidewalls. The strong secondary flows generated by the ramp and cowl shocks in the corner regions merge along the sidewalls as shown in the fourth plane from the right, and then bulge outward into the interior flow field. The last three planes of Figure 10 are shown in Figure 11. The thinning of the corner boundary layers is evident in this figure as well as the outward bulging of the flow along the sidewalls. In the first plane from the right, the shock waves, seen as the two sets of horizontal lines in the center of the plane, have just crossed. In the second plane the ramp shock has reflected off the cowl and the cowl shock is reflecting off the ramp. Between the second and last planes the ramp shock hits the ramp surface about 2 inches downstream of the cowl shoulder, reflects and merges with the cowl shock. In the last plane the merged shocks which have not yet reached the cowl surface are visible as the closed contour at the top of the plane.

The three-dimensional flow through the Generic Option 2 inlet was calculated using the PNS turbulent analysis at Mach 11.3. The computational grid for this case was 750 x 80 x 60. Figures 12 and 13 present Mach number contours for this calculation, demonstrating the three dimensional nature of the flow field. Flow is from right to left in these two figures. The concentration of lines near a physical surface indicate the presence of a boundary layer, while concentrations away from physical surfaces indicate shock locations. At the farthest upstream station ahead of the inlet, at the right, one can discern the predicted boundary layer height on the simulated forebody. As the flow proceeds into the inlet at the second plane from the right, boundary layers are generated on the sideplates and ramp surfaces. The shock wave generated by the ramp is just at the edge of the boundary layer at this station. Proceeding into the inlet, the third plane from the right shows the shock waves generated by the ramp and cowl as horizontal lines, while the sidewall boundary layer displacement has generated weak shocks near the sidewalls shown as vertical lines. The shocks generated by the compression surface glance across the boundary layers on the sidewalls producing a characteristic thickening of the boundary layer near the shock and thinning of the boundary layer in the corners. Strong secondary flows are generated by the shock wave/boundary layer interaction which affect the flow downstream in the inlet.

In Figure 13 only the last three planes of the inlet flow field are shown. The viewpoint has been changed from the previous figure. One now views the computed flow field from outside and behind the inlet, looking through the near sidewall. The plane at the right is the same as the last plane of the previous figure. The compression shocks from the ramp and cowl appear as horizontal lines. The swirling lines around the shocks indicate the boundary layers which have grown on the wedges and sidewalls and which have been highly distorted by interactions with the compression shocks. The low energy flow of the sidewall boundary layer has been swept up the sidewall by the ramp shock and down the sidewall by the cowl shock. Near the center of the sidewall these two secondary flows collide. As the flow proceeds downstream to the center plane, the shock waves cross and are distorted by interaction with the sidewall boundary layer and the expansion fan on the ramp surface. At this station, the ramp shock is reflecting from the cowl surface and the cowl shock is seen as the horizontal line through the middle of the plane. Vortices generated by the shock/boundary layer interactions have pulled away from the sidewall while interacting with each other. Proceeding to the last plane on the left, the expansion generated on the lower surface causes a strong pressure gradient from top to bottom. Low energy flow along the sidewall moves into the corner formed by the sidewall and the ramp surface. As the shock wave created by the ramp and reflected from the cowl strikes the ramp surface, just under the cowl shoulder, the low energy flow in the corner separates. The PNS analysis cannot be made to proceed farther due to the magnitude of the separation in the lower corners, vortical flow near the sidewalls and thick boundary layers on both the ramp and cowl surfaces.

The primary difference between the two calculations is that the turbulent flow at Mach 11.3 separates while the laminar flow at Mach 12.25 remains attatched throughout the inlet. A possible explanation for this difference is the locations of the shock wave ramp intersection in the constant area portion of the inlet. The shock wave for the turbulent calculation hits the ramp at a location just under the cowl shoulder, whereas the shock wave for the laminar case hits the ramp surface several inches further downstream. The expansion over the ramp shoulder causes low momentum flow to be drawn into the ramp-sidewall corner. The turbulent Mach 11.3 flow seperates in the ramp-sidewall corner before the sidewall flow has been influenced by the cowl shoulder. The higher Mach number in the laminar cases causes the shock wave angles to be decreased and the shock intersection in the constant area portion of the inlet to be moved further downstream. The flow of low energy flow into the ramp-sidewall corner is decreased buy the cowl shoulder expansion thus causing the flow to remain attatched.

CONCLUSIONS

The hypersonic flow studied experimentally by the McDonnell Douglas corporation has been analyzed using two different CFD models. Three-dimensional laminar NS calculations were compared with the experimental data. These calculations demonstrated a strong three-dimensional flow effect in the inlet; static pressure distributions along the centerline were in much closer agreement with the experiment for the three-dimensional calculations than for the two-dimensional ones. The three-dimensional flow field calculated using PARC3D exhibited the strong secondary flows generated by shock/boundary layer interactions. The turbulent 3D PNS analysis at Mach 11.3 indicated that the inlet would experience strong secondary flows generated by shock/boundary layer interactions and would probably experience large flow separations in the corners formed by the compression surface and sidewall. Separations in this part of the inlet are critical and could lead to inlet unstart by generating strong normal shocks near the separation bubble. It appears that strongly three-dimensional flows exist in this class of rectangular internal-compression inlets in this speed regime. Controlling these interactions presents a major challenge for high speed air-breathing propulsion.

REFERENCES

1. Cooper, G.K., Jordan, J.L., and Phares, W.J., "Analysis Tool for Application to Ground Testing of Highly Underexpanded Nozzles", AIAA 87-2015, 1987.

2. Buggeln, R.C., McDonald, H., Levy, R., and Kreskovsky, J.P., "Development of a Three-Dimensional Supersonic Inlet Flow Analysis," NASA CR-3218. 1980.

3. Kim, S.C., and Harloff, G.J., "Hypersonic Turbulent Wall Boundary Layer Computations", NASA CR 182147, May 1988.

4. Harloff, G.J., Lai, H.T., and Nelson, E.S., "Two-Dimensional Viscous Flow Computations of Hypersonic Scramjet Nozzle Flowfields at Design and Off Design Conditions', NASA CR 182150, June 1988.

5. Hsu, A.T., "The Effect of Adaptive Grid on Hypersonic Nozzle Flow Calculations", AIAA 89-0006, January, 1989.

6. Hsu, A.T and Liou, M.S., "A Computational Analysis of Under Expanded Jets in the Hypersonic Regime", NASA TM 101319, August 1988.

7. Reddy, D.R., and Harloff, G.J., "Three-Dimensional Viscous Flow Computations and High Area Ratio Nozzles for Hypersonic propulsion", AIAA paper 88-0474, January, 1988.

8. Lai, H.T., and Nelson, E.S., "Comparison of 3-D Computation and Experiment for Non-Axisymmetric Nozzles", AIAA 89-0007, January 1989.

9. Harloff, G.J. , and Lytle, J.K. "Three-Dimensional Viscous Flow Computations of a Circular Jet in Subsonic and Supersonic Cross Flow. NASA CR 182153, July, 1988.

10. Smith, G.E., and Benson, T.J., "PNS Calculations for 3-D Hypersonic Corner Flow with Two Turbulence Models", AIAA 88-2958, July, 1988.

11. Benson, T.J., Liou, M-F, and Smith, G.E., "Viscous Analysis of M=11.3 McDonnell Douglas Inlet", Fourth NASP Symposium, Monterey, California, Paper No. 100, February 1988.

12. Benson, T.J., "Three-Dimensional Viscous Calculations of Flow in a Mach 5.0 Hypersonic Inlet," AIAA Paper 86-1461, June 1986.

13. Beam, R. and Warming, R.F., "An Implicit Finite-Difference Algorithm for Hyperbolic Systems in Conservation Law form', Journal of Computational Physics, Vol 22, No. 1, Sept 1976, pp. 87-110.

14. Jameson, A., Schmidt, W. and Turkel, E., "Numerical Solutions of the Euler Equations by Finite Volume Method Using Runge-Kutta Time Stepping Schemes", AIAA 81-1259, 1981.

15. Pulliam, T.H., "Euler and Thin Layer Navier-Stokes Codes: ARC2D, ARC3D", Notes for Computational Fluid Dynamics User's Workshop, The University of
Tennessee Space Institute, Tullahoma, Tennessee, March 12-16, 1984.

16. Pulliam, T.H., and Steger, J.L., "Implicit Finite-Difference Simulations of Three Dimensional Compressible Flow.", AIAA Journal, Vol. 18, February 1980, pp. 159-167.

17. "National Aerospace Plane Generic Option 2 Experimental Data Base/CFD Code Validation," McDonnell Douglas, Contract F-33657-C-2126, May 1988.

18 Cosner, R., private communication, McDonnell Douglas, St. Louis Missouri.

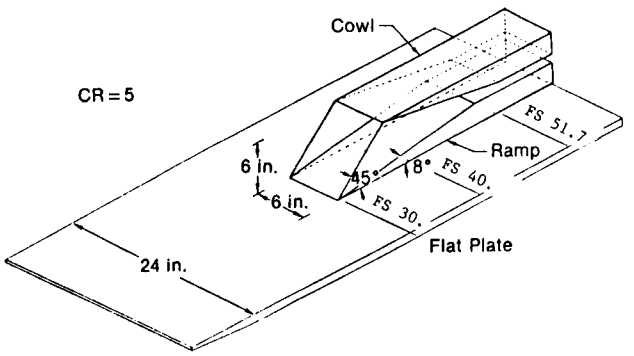

Figure 1. Generic Option 2 Geometry

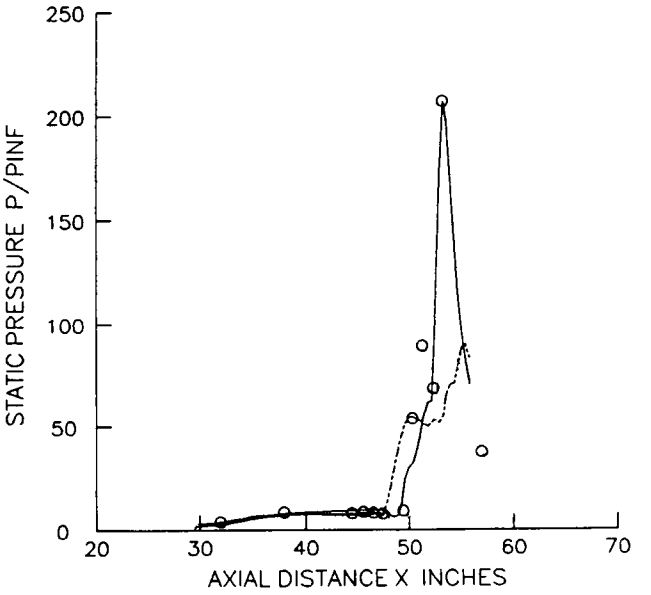

Figure 2. Centerline Pressure Distribtution on Ramp Surface

——— PARC3D
○ ○ Experimental Data
-·-·- PARC2D

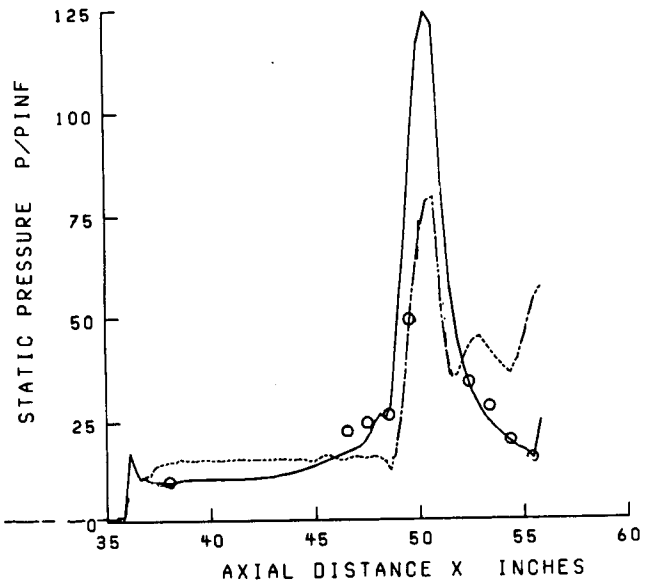

Figure 3. Centerline Pressure Distribution on Cowl Surface

——— PARC3D
○ ○ Experimental Data
-·-·- PARC2D

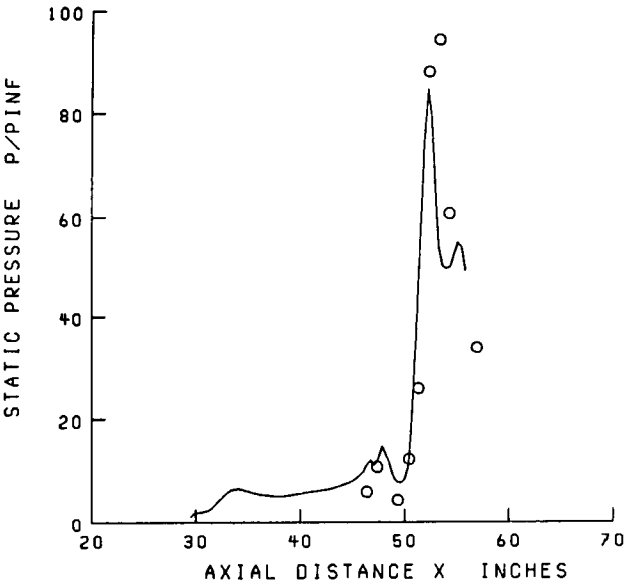

Figure 4. Outboard Pressure Distribution on Ramp Surface

——— PARC3D
○ ○ Experimental Data

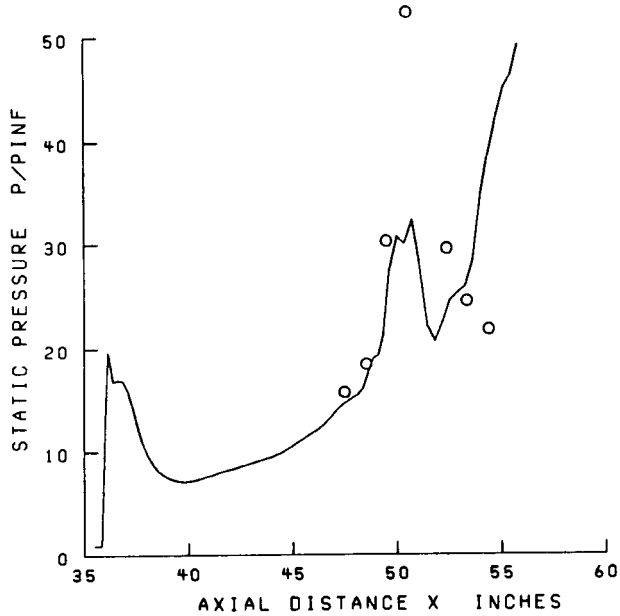

Figure 5. Outboard Pressure Distribtution on Cowl Surface

PARC3D
Experimental Data

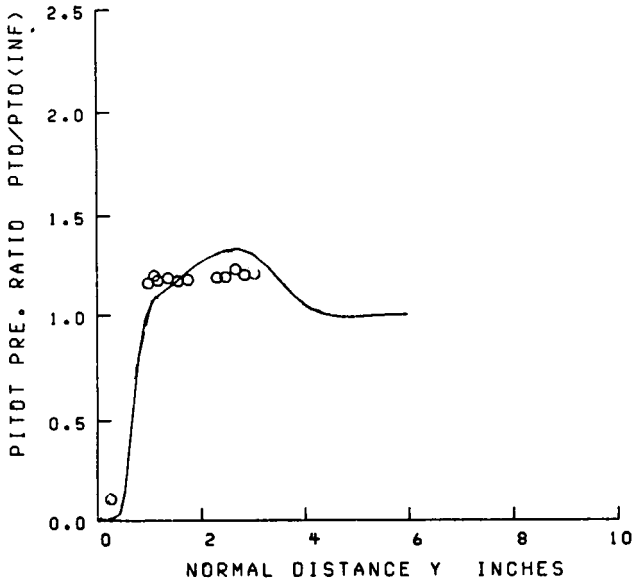

Figure 6. Pitot Pressure Profile at F-S 30.0

PARC3D
Experimental Data

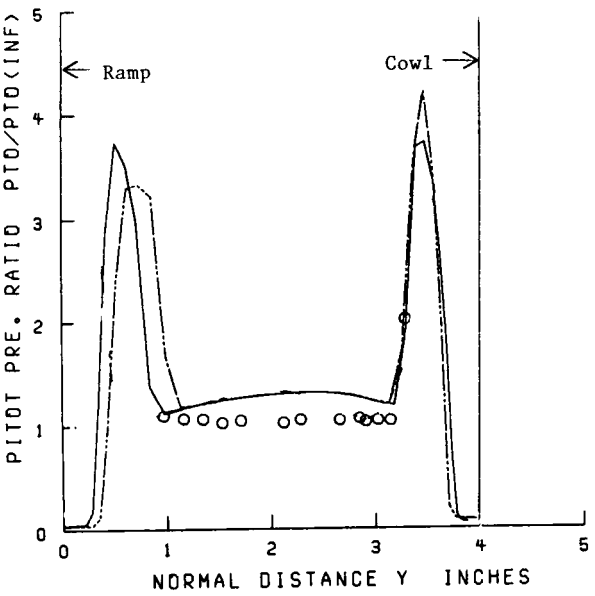

Figure 7. Pitot Pressure Profile at F-S 40.0 (Centerline)

PARC3D
Experimental Data
PARC2D

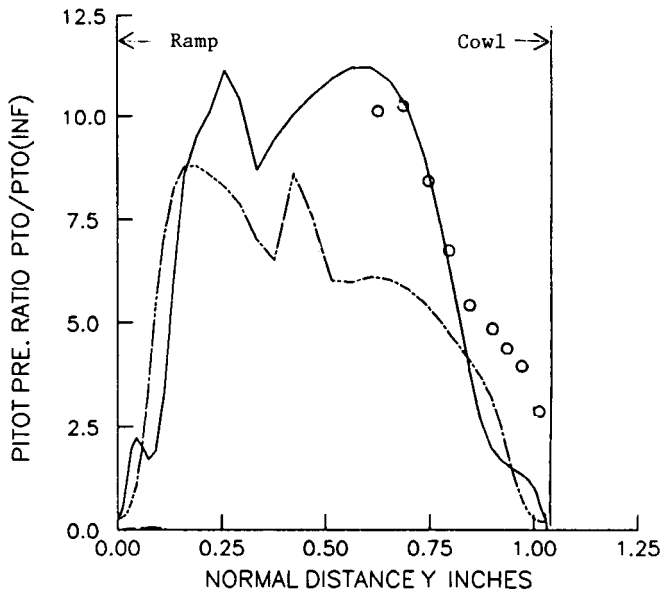

Figure 8. Pitot Pressure Profile at F-S 51.7 (Centerline)

PARC3D
Experimental Data
PARC2D

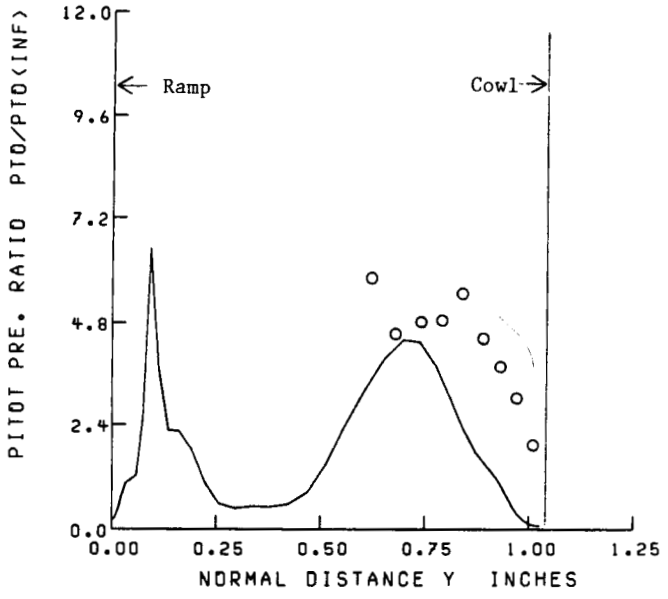

Figure 9. Pitot Pressure Profile at F-S 51.7 (Outboard)

——— PARC3D
○ ○ Experimental Data

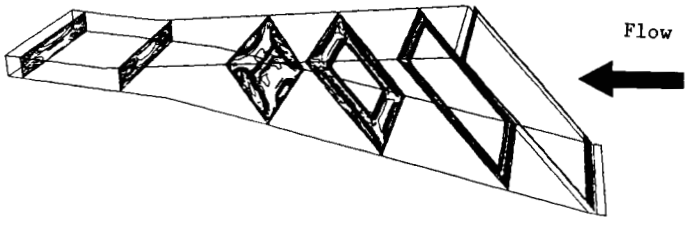

Figure 10. Mach Number Contours: PARC3D

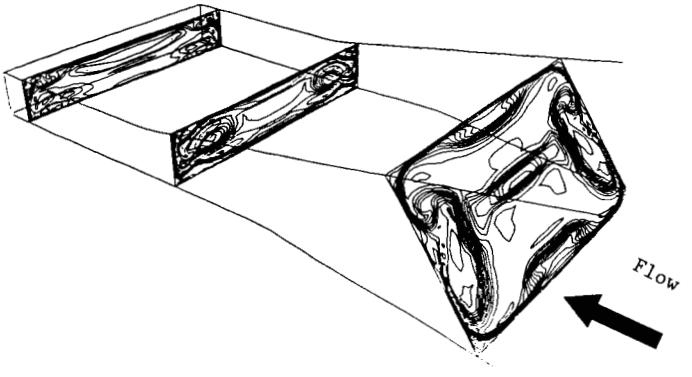

Figure 11. Mach Number Contours: PARC3D (Close Up)

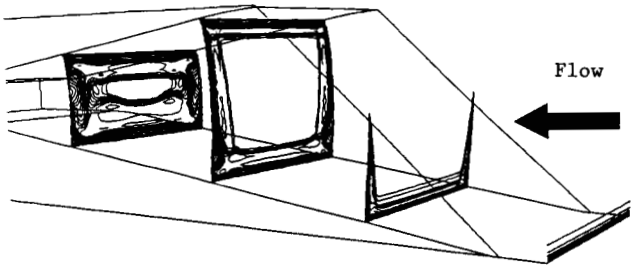

Figure 12. Mach Number Contours: PEPSIS

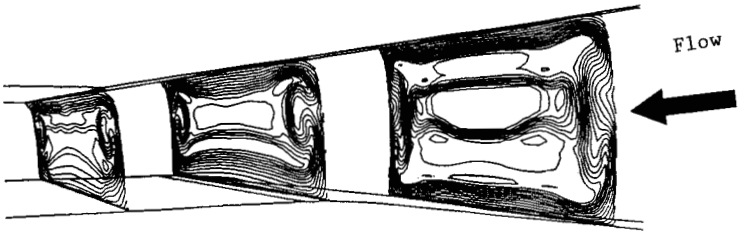

Figure 13. Mach Number Contours: PEPSIS (Closeup)

NASA
National Aeronautics and Space Administration

Report Documentation Page

1. Report No.	2. Government Accession No.	3. Recipient's Catalog No.
NASA TM-101474 AIAA-89-0004		

4. Title and Subtitle	5. Report Date
Three Dimensional Viscous Analysis of a Hypersonic Inlet	
	6. Performing Organization Code

7. Author(s)	8. Performing Organization Report No.
D.R. Reddy, G.E. Smith, M.-F. Liou, and T.J. Benson	E-4592
	10. Work Unit No. 763-01-21

9. Performing Organization Name and Address	11. Contract or Grant No.
National Aeronautics and Space Administration Lewis Research Center Cleveland, Ohio 44135-3191	
	13. Type of Report and Period Covered Technical Memorandum
12. Sponsoring Agency Name and Address	14. Sponsoring Agency Code
National Aeronautics and Space Administration Washington, D.C. 20546-0001	

15. Supplementary Notes

Prepared for the 27th Aerospace Sciences Meeting sponsored by the American Institute of Aeronautics and Astronautics, Reno, Nevada, January 9-12, 1989. D.R. Reddy, G.E. Smith, and M.-F. Liou, Sverdrup Technology, Inc., NASA Lewis Research Center Group, Cleveland, Ohio 44135; T.J. Benson, NASA Lewis Research Center.

16. Abstract

The flow fields in supersonic/hypersonic inlets are currently being studied at NASA Lewis Research Center using two- and three-dimensional full Navier-Stokes and Parabolized Navier-Stokes solvers. These tools have been used to analyze the flow through the McDonnell Douglas Generic Option 2 inlet which has been tested at Calspan in support of the National Aerospace Plane Program. Comparisons between the computational and experimental results are presented. These comparisons lead to better overall understanding of the complex flows present in this class of inlets. The aspects of the flow field emphasized in this work are the three-dimensional effects, the transition from laminar to turbulent flow, and the strong nonuniformities generated within the inlet.

17. Key Words (Suggested by Author(s))	18. Distribution Statement
Computational Fluid Dynamics Hypersonic flow Three-dimensional full Navier-Stokes solver Shock-boundary layer interaction	Unclassified – Unlimited Subject Category 02

19. Security Classif. (of this report)	20. Security Classif. (of this page)	21. No of pages	22. Price*
Unclassified	Unclassified	8	A02

*For sale by the National Technical Information Service, Springfield, Virginia 22161